

Magnetic structure and spin excitations in BaMn₂Bi₂

S. Calder,^{1,*} B. Sapiro,² H. B. Cao,³ J. L. Niedziela,¹ M. D. Lumsden,¹ A. S. Sefat,² and A. D. Christianson¹

¹*Quantum Condensed Matter Division, Oak Ridge National Laboratory, Oak Ridge, TN 37831.*

²*Materials Science and Technology Division, Oak Ridge National Laboratory, Oak Ridge, TN 37831.*

³*Instrument and Source Division, Oak Ridge National Laboratory, Oak Ridge, TN 37831.*

(Dated: August 16, 2021)

We present a single crystal neutron scattering study of BaMn₂Bi₂, a recently synthesized material with the same ThCr₂Si₂-type structure found in several Fe-based unconventional superconducting materials. We show long range magnetic order, in the form of a G-type antiferromagnetic structure, to exist up to 390 K with an indication of a structural transition at 100 K. Utilizing inelastic neutron scattering we observe a spin-gap of 16 meV, with spin-waves extending up to 55 meV. We find these magnetic excitations to be well fit to a J_1 - J_2 - J_c Heisenberg model and present values for the exchange interactions. The spin wave spectrum appears to be unchanged by the 100 K structural phase transition.

I. INTRODUCTION

The discovery of unconventional superconductivity in Fe-based materials has stimulated intense interest in the condensed matter physics community, and offers a new system, with the same square planar crystal motif as the cuprates, in which to investigate the underlying mechanism of unconventional superconductivity¹⁻³. Driven by the initial discovery of superconductivity several new Fe-based materials have been uncovered, for example the 1111 phase ($R\text{FeAsO}$ with R = rare earth), 111 phase ($A\text{FeAs}$ with A = alkali metal), 11 phase (FeTe or FeSe), 122 phase ($A\text{Fe}_2\text{As}_2$), and FeSe_{122} phase ($A\text{Fe}_2\text{Se}_2$)^{2,3}. The FeAs (or FeSe) layers are the common ingredient and unlike the cuprates it is possible to dope the Fe site and attain superconductivity. As a consequence much work has been done on this, particularly in the 122 phase.

Recent interest has also focused on complete substitution of the Fe ion in the 122-type structure as an avenue to both search for new classes of superconducting materials or probe why no superconductivity is attained despite often similar physics. One pertinent example being SrCo_2As_2 that shows many similar features to the Fe-based 122 materials, but as yet no superconductivity has been uncovered upon doping from the cobalt parent side⁴. Additionally the chromium based material BaCr_2As_2 was shown to host itinerant antiferromagnetism that differs from the Fe-122 materials that remains upon doping and prohibits superconductivity^{5,6}.

Directly related to our investigation is the Mn-122 material BaMn_2As_2 that shows alternative behavior to both Co and Fe-122 materials as well as the cuprates. BaMn_2As_2 is a G-type antiferromagnet (AFM), $T_N=625$ K, with no structural transition in the magnetic phase^{7,8}. Investigations of BaMn_2As_2 have indicated properties in the intermediate regime between those of the itinerant $A\text{Fe}_2\text{As}_2$ antiferromagnets and the local moment antiferromagnetic insulator La_2CuO_4 parent superconductors. Indeed doping BaMn_2As_2 in the form $\text{Ba}_{1-x}\text{K}_x\text{Mn}_2\text{As}_2$ has been shown to result in an antiferromagnetic local moment metal⁹. Therefore it has been suggested

that Mn-122 compounds may be well placed to act as a bridge between Fe and Cu based unconventional superconductors².

Ref. 10 reported the growth and characterization of single crystals of the new Mn-122 material, BaMn_2Bi_2 ¹⁰ the first bismuthide with ThCr₂Si₂-type structure (space group $I4/mmm$ with $a=4.4902(3)$ Å and $c=14.687(1)$ Å). BaMn_2Bi_2 is insulating with a small band gap of $E_g = 6$ meV, with metallic behavior achieved via hole doping with 10% K substitution on the Ba site¹⁰. Susceptibility measurements revealed an anomaly around 400 K consistent with magnetic ordering, with an additional apparent anomaly around 100 K that also corresponds to an upturn in the resistivity¹⁰.

BaMn_2Bi_2 shows similar properties to BaMn_2As_2 and therefore may be similarly placed to act as a bridge between Fe and Cu based unconventional superconductors. Additionally BaMn_2Bi_2 offers an alternative to arsenic based materials and is amenable to the growth of suitably large single crystals for neutron scattering. Here we report the results of a single crystal neutron diffraction investigation of BaMn_2Bi_2 through both the 400 K and 100 K anomalies observed from bulk measurements. We then extend our exploration of the physical properties of BaMn_2Bi_2 to a study of the spin excitation spectrum by means of inelastic neutron scattering measurements. Our results support the postulate that the Mn-122 series hosts magnetic and insulating properties intermediate between Fe and Cu based materials and we utilize our single crystal inelastic neutron scattering results to provide detailed information on the magnetic exchange interactions and spin gap.

II. EXPERIMENTAL METHODS

A detailed description of the single crystal growth and characterization of BaMn_2Bi_2 is presented in Ref. 10. Single crystal neutron scattering measurements were performed on the Four-circle diffractometer (HB-3A) at the High Flux Isotope Reactor at ORNL. A single crystal of ~100 mg was measured in the temperature range 4 K

to 400 K and the data refined using Fullprof to obtain crystal and magnetic structures. To attain a suitable mass (~ 3 grams) for inelastic neutron scattering measurements five single crystals were coigned to within 1° in the (HHL) scattering plane. Utilizing the ARCS spectrometer at the SNS, ORNL, inelastic neutron measurements were performed at 4 K and 120 K with incident energies of 60, 100, 120, 250 and 500 meV. To examine the spin excitations in all reciprocal lattice directions the sample was rotated by 90° in 1° for measurements with an incident energy of 100 meV. The different angular data was combined and subsequent cuts performed with the Horace software¹¹. The instrument resolution varies with energy transfer and this was accounted for in our fitting of the data through the use of an analytical function described in Ref. 12. The inelastic energy resolution at an energy transfer of 50 meV is 1.56 meV for 100 meV incident energy.

III. RESULTS AND DISCUSSION

A. Magnetic and nuclear structure of BaMn_2Bi_2

We begin our investigation of BaMn_2Bi_2 with single crystal Four-circle neutron diffraction measurements. We performed measurements on several different nuclear reflections and found the refined structure to be consistent with the previously reported powder x-ray measurements¹⁰. From susceptibility measurements there is an anomaly around 400 K, attributed magnetic ordering¹⁰. We observed intensity at the (101) reflection, a reflection forbidden by the nuclear space group symmetry but consistent with AFM long range order. Indeed this defines the propagation vector for BaMn_2Bi_2 with space group $I4/mmm$ in the body centered tetragonal notation, in primitive tetragonal notation the propagation vector transforms to $(\frac{1}{2}, \frac{1}{2}, \frac{1}{2})$. Following the temperature evolution of the intensity at the (101) reflection position from 4 K to 400 K we observe a magnetic transition at $T_N = 387.2(4)$ K, shown in Fig. 1. Considering the intensity of magnetic reflections in different Brillouin zones at 4 K within a model based on equal populations of domains for tetragonal symmetry, and normalizing to the nuclear reflections, we were able to define the magnetic structure in BaMn_2Bi_2 as being G-type AFM, with the spins aligned along the c -axis. The ordered moment at 4 K is $3.83(4)\mu_B/\text{Mn}$, reduced from the $5\mu_B/\text{Mn}$ expected for the high-spin $S=5/2$ of Mn^{2+} , nevertheless closer to a local moment description relative to the itinerant Fe-based superconductors. The magnetic structure, and within error the ordered moment, is the same as for the related Mn-122 BaMn_2As_2 ⁷.

Both susceptibility and resistivity measurements on BaMn_2Bi_2 suggest a further transition around 100 K¹⁰. The behavior of the (101) magnetic reflection in Fig. 1(a), however, shows no observable change in the magnetic structure in this region. Fig. 1(b) shows the nuclear (008)

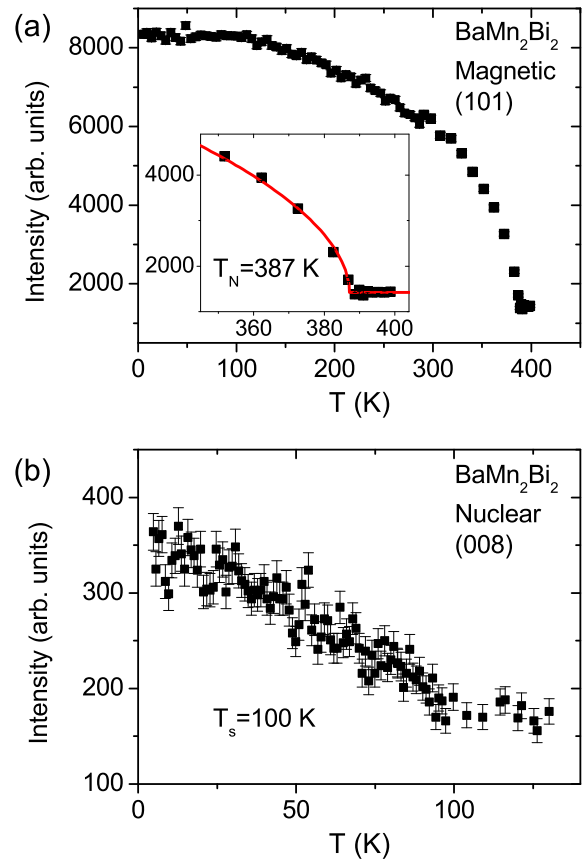


FIG. 1. Single crystal neutron scattering measurements on BaMn_2Bi_2 . (a) Magnetic ordering occurs at (101) reflections, with the onset at 387.2(4) K. (b) A subtle structural transition is indicated by the change in the nuclear (008) reflection below 100 K.

reflection, with an anomaly at the same temperature as that observed in bulk measurements. Such a change is indicative of a subtle tetragonal to orthorhombic transition that is not observable as a peak splitting due to the instrument resolution, but would be manifested in a change in the extinction and therefore the measured intensity of a nuclear reflection. A tetragonal to orthorhombic structural change is observed in several Fe-122 parent superconductors and is perhaps a prerequisite for attaining superconductivity, however no structural change in the magnetic ordered phase has been observed in the related BaMn_2As_2 .

B. Spin excitations of BaMn_2Bi_2

We now consider the magnetic excitations through a single crystal inelastic neutron scattering experiment on ARCS with the aim of finding the exchange interactions and observing any spin-gap, in addition to comparing excitations through the apparent 100 K structural transition. We performed an initial survey using incident en-

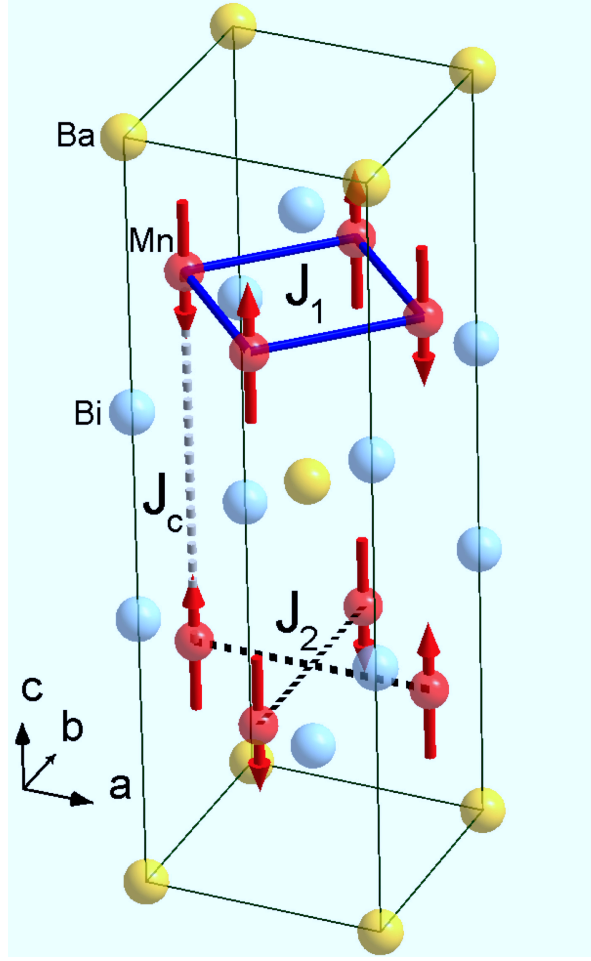


FIG. 2. Crystal structure of BaMn_2Bi_2 with G-type AFM ordering of the Mn-ions shown within the nuclear unit cell. The exchange interactions used in the model Hamiltonian correspond to J_1 (ab-plane nearest neighbor), J_2 (ab-plane next nearest neighbor) and J_c (c-axis nearest neighbor).

ergies of $E_i=60, 120, 250$ and 500 meV with the incident beam along the c -axis. This allowed us to find the top of the spin excitations at ~ 60 meV and rule out any higher energy spin waves. With the spin excitations residing around 60 meV and below we chose an $E_i=100$ meV to map out the low Q Brillouin zones and performed cuts along high symmetry directions. Constant energy cuts are shown in Fig. 3(a)-(h) that follow the evolution of the low energy excitations.

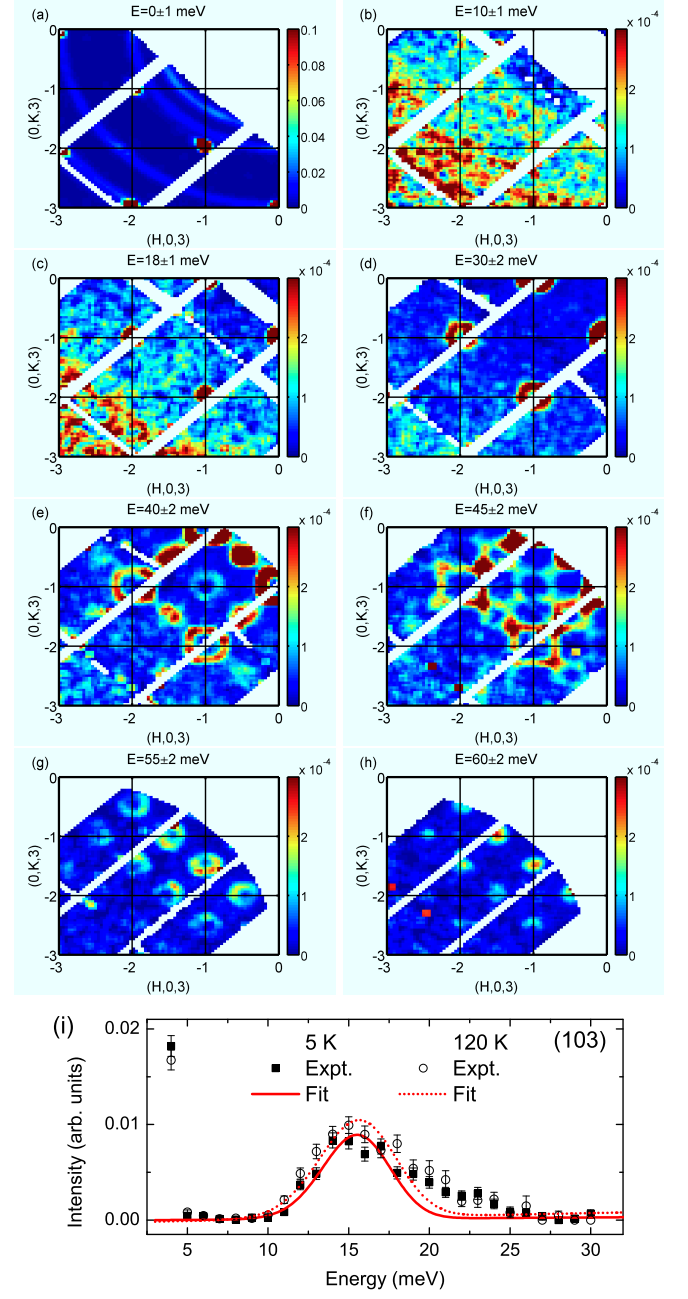


FIG. 3. Inelastic neutron scattering measurements on single crystals of BaMn_2Bi_2 with an incident energy of 100 meV. (a)-(h) Constant energy cuts projected onto the (H,K) plane for fixed $L=3$. The scale corresponds to intensity in arbitrary units. Excluding the $E=0$ meV slice the scale remains fixed for each plot. (i) Constant $q=(1,0,3)$ cut from the magnetic Bragg reflection in the range $(0.93 < H < 1.07, -0.07 < K < 0.07, 2.93 < L < 3.07)$ to reveal the spin-gap. The fit is performed excluding the region around 20 meV to remove background.

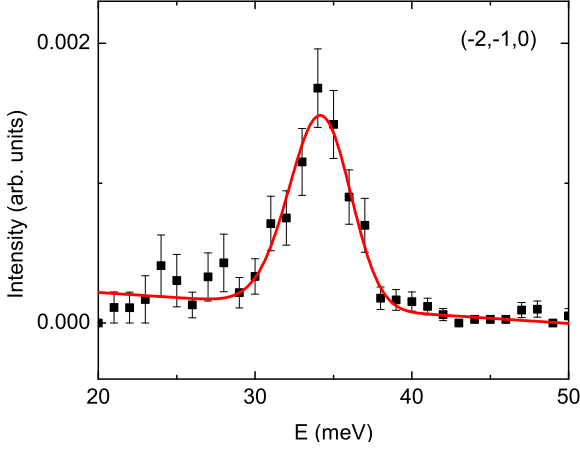


FIG. 4. Energy variation showing the width of the excitation through the zone boundary at $(-2,-1,0)$ at 4 K. The fit is a gaussian convolved with the instrument energy resolution.

Familiar spin-wave cones are seen to develop centered on the magnetic Bragg points (Fig. 3(a)-(d)), with overlapping excitations near the maximum of the branches (Fig. 3(e)-(f)). The lack of any Q-dependent scattering in Fig. 3(b) at 10 meV indicates the existence of a spin-gap in BaMn_2Bi_2 . This is confirmed by an energy cut from the elastic magnetic Bragg reflection position (103), as shown in Fig. 3(i) where a distinct energy gap is observed well within the instrumental energy resolution of 2.7 meV at 5 meV energy transfer. No change in the gap is apparent through 100 K, where we observed a subtle structural transition from our single crystal neutron diffraction. In order to fit the data we exclude the region around 20 meV where background aluminum scattering occurs and fit the resulting profile to a gaussian convoluted with the instrument resolution to give an energy gap of $E_g = 16.29(26)$ meV at 5 K. The existence of a spin-gap between $E_g = 6$ to 9 meV is a general feature of the inelastic neutron spectrum of parent Fe-122 materials^{13,14}, with debate existing as to the importance and consequence on the emergence of superconductivity. No spin-gap is reported from the inelastic neutron scattering results of BaMn_2As_2 ⁸. This may be a consequence of only polycrystalline BaMn_2As_2 being synthesized or conversely point to different physics between the Mn-122 materials.

Figure 4 shows the energy variation and width through the spin waves at the zone boundary. The zone boundary energy is determined to be 34.2(3) meV, with a FWHM of 2.42(8) meV. With an instrument resolution at 34 meV of 1.9 meV this indicates sharp excitations, in contrast to what is observed for the Fe-122 materials, such as BaFe_2As_2 ¹⁵, that show diffuse scattering at the zone boundary. This distinction is likely an indication of a local moment picture being more instructive for BaMn_2Bi_2 as compared to the itinerant Fe-122 parent superconductors.

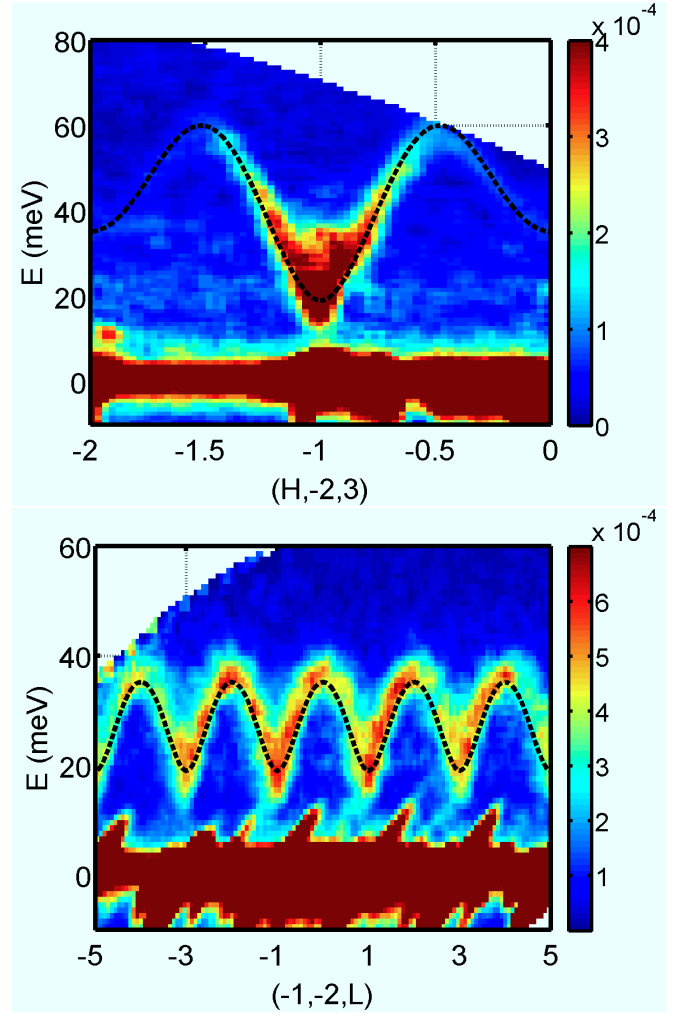


FIG. 5. Inelastic neutron scattering measurements on single crystals of BaMn_2Bi_2 show well defined dispersions along high symmetry directions. The intensity scale is in arbitrary units. The black dashed lines corresponds to the calculated dispersion relation using exchange interactions as described in the text.

Theoretically the spin-gap is accounted for as a breaking of the Heisenberg spin rotation symmetry due to single ion anisotropy in the model Hamiltonian and we use this in our fitting method. We start from the Heisenberg Hamiltonian that has proven effective for the low energy excitations in the Fe-122 parent superconducting materials such as CaFe_2As_2 and BaFe_2As_2 ^{16,17}:

$$H = \sum_{\langle ij \rangle} (J_{ij}) S_i \cdot S_j + \sum_{\langle i \rangle} D(S_z^2)_i \quad (1)$$

where J_{ij} are exchange constants. We consider the ab -plane nearest neighbor (J_1) and next nearest neighbor (J_2) interactions as well as the interaction from the c -axis nearest neighbor (J_C), shown schematically in Fig. 2, with the spin wave dispersion given by

$$E(q) = \sqrt{A(q)^2 - B(q)^2} \quad (2)$$

In order to compare the exchange interactions with the related Mn-122 material BaMn₂Bi₂ and remain in tetragonal notation we use the form of dispersion presented by Johnston *et al.* in Ref. 8, with the addition of a single ion-anisotropy term (D) due to the observed spin-gap, with

$$A(q) = 2 + \frac{J_c}{J_1} - \frac{J_2}{J_1} [2 - \cos(q_x a) - \cos(q_y a)] + D \quad (3)$$

$$B(q) = \cos([q_x + q_y] \frac{a}{2}) + \cos([q_x - q_y] \frac{a}{2}) + \frac{J_c}{J_1} \cos(\frac{q_z c}{2}) \quad (4)$$

where a and c are the tetragonal lattice constants of BaMn₂Bi₂ and the spin-wave energy is in units of SJ_1 . This dispersion relationship is equivalent to those in Refs. 16 and 17. For the case of G-type AFM with spins along the c -axis the exchange interactions must satisfy the constraints that J_1 and J_c are positive and $J_1 > 2J_2$.

Figure 5 shows the measured spin wave dispersions projected onto high symmetry directions in BaMn₂Bi₂. To obtain the exchange interaction values we took constant q cuts with varying energy transfer through the dispersions and fit the results with a gaussian convolved with the instrument resolution to obtain the position of the dispersions. The results were then modeled with the dispersion relationship, equation (2), along both H and L directions to find the following unique set of exchange interactions that describe the magnetic spin excitations: $SJ_1 = 21.7(1.5)$, $SJ_2 = 7.85(1.4)$, $SJ_c = 1.26(0.02)$, $SJ_s = 0.046(0.006)$. The exchange values are consistent with the constraints for G-type AFM ordering. Within the resolution of our measurements we do not find any change in exchange interactions between 4 K and 120 K.

Comparing the exchange interactions with those of BaMn₂As₂ reported in Ref. 8 shows a reduction in all values in BaMn₂Bi₂, and a lowering of the top of the observed excitations from 70 meV to 55 meV. The lowering of the excitations may be anticipated from the overall reduction in magnetic ordering temperature of ~ 200 K from BaMn₂As₂ to BaMn₂Bi₂. The largest relative difference between the exchange interactions is the reduction of the interaction along the c -axis from 3 meV (BaMn₂As₂) to 1.26 meV (BaMn₂Bi₂). This may be explained in part as a consequence of the increase in the interplanar separation from 6.7 Å for the MnAs layers in BaMn₂As₂ to 7.3 Å for the MnBi layers in BaMn₂Bi₂ due to the c -lattice constant increase from 13.4149(8) Å (BaMn₂As₂) to 14.687(1) Å (BaMn₂Bi₂). However, the relative change of $\sim 8\%$ is the same as the reduction in the Mn-Mn interplanar distance between BaMn₂Bi₂ and BaMn₂As₂, suggesting further mechanism are important, such as the changes induced by the bismuth ion over the arsenic ion in the lattice.

Considering results for the exchange interactions in the J_1 - J_2 - J_c model for CaFe₂As₂^{13,18,19}, BaFe₂As₂^{18,20} and SrFe₂As₂^{14,18} we find reduced values for all exchange interactions in the form SJ in BaMn₂Bi₂ apart from a lower J_c value in BaFe₂As₂, however comparable single-ion anisotropy values. Therefore, in general, it appears the spin-waves and exchange interactions in BaMn₂Bi₂ are lower in energy compared to 122 materials, even though the magnetic ordering temperature lies between BaMn₂As₂ and the Fe-122 materials. The overall divergence of excitations energy and width, despite similarities such as the observed spin gap and structural transition in the magnetic phase, is a reflection of the differing underlying physical properties between BaMn₂Bi₂ and Fe-122 materials and further investigations via doping would be of interest to follow the evolution of the excitations in this Mn-122 material.

IV. CONCLUSIONS

Neutron scattering measurements on single crystals have revealed BaMn₂Bi₂ forms G-type AFM at 390 K with spins aligned along the c -axis. We find an ordered moment of $\sim 75\%$ compared to the expected spin-only value indicating possible hybridization and divergence from pure local moment behavior, however BaMn₂Bi₂ appears to reside much closer to the local moment limit than itinerant Fe-122 systems. Our elastic neutron scattering suggests BaMn₂Bi₂ undergoes a subtle structural transition, similar to the Fe-122 materials but distinct from the related Mn-122 material BaMn₂As₂. A general feature of Fe-122 systems is the existence of a spin-gap as observed in inelastic neutron measurements, while the underlying relationship, if any, to superconductivity remains an open question. Our measurements on gram sized single crystals reveal well defined spin waves and a gap of 16 meV in the low energy excitations in BaMn₂Bi₂, not seen in BaMn₂As₂, that remains unchanged in the magnetic regime from 5 K to 120 K. Indeed the spin excitations show no apparent change through the structural transition. Applying a J_1 - J_2 - J_c Heisenberg model accounts well for the spin excitations and shows a lower energy scale compared to both BaMn₂As₂ and the Fe-122 materials. Overall our results are consistent with the postulate that the Mn-122 materials hosts intermediate properties between the local moment antiferromagnet insulating cuprate parent materials and itinerant antiferromagnetic Fe systems. Therefore in the context of investigating phenomena related to unconventional superconductivity BaMn₂Bi₂ appears to be well suited as a potential new bridging material.

ACKNOWLEDGMENTS

This research at ORNL's High Flux Isotope Reactor and Spallation Neutron Source was sponsored by the Sci-

entific User Facilities Division, Office of Basic Energy Sciences, U.S. Department of Energy. Research was sup-

ported by the U.S. Department of Energy (DOE), Basic Energy Sciences (BES), Materials Sciences and Engineering Division (BS, AS).

-
- * caldersa@ornl.gov
- ¹ Y. Kamihara, T. Watanabe, M. Hirano, and H. Hosono, *Journal of the American Chemical Society*, **130**, 3296 (2008).
 - ² D. C. Johnston, *Advances in Physics*, **59**, 803 (2010).
 - ³ M. D. Lumsden and A. D. Christianson, *Journal of Physics: Condensed Matter*, **22**, 203203 (2010).
 - ⁴ W. Jayasekara, Y. Lee, A. Pandey, G. S. Tucker, A. Sapkota, J. Lamsal, S. Calder, D. L. Abernathy, J. L. Niedziela, B. N. Harmon, A. Kreyssig, D. Vaknin, D. C. Johnston, A. I. Goldman, and R. J. McQueeney, *Phys. Rev. Lett.*, **111**, 157001 (2013).
 - ⁵ D. J. Singh, A. S. Sefat, M. A. McGuire, B. C. Sales, D. Mandrus, L. H. VanBebber, and V. Keppens, *Phys. Rev. B*, **79**, 094429 (2009).
 - ⁶ K. Marty, A. D. Christianson, C. H. Wang, M. Matsuda, H. Cao, L. H. VanBebber, J. L. Zarestky, D. J. Singh, A. S. Sefat, and M. D. Lumsden, *Phys. Rev. B*, **83**, 060509 (2011).
 - ⁷ Y. Singh, M. A. Green, Q. Huang, A. Kreyssig, R. J. McQueeney, D. C. Johnston, and A. I. Goldman, *Phys. Rev. B*, **80**, 100403 (2009).
 - ⁸ D. C. Johnston, R. J. McQueeney, B. Lake, A. Honecker, M. E. Zhitomirsky, R. Nath, Y. Furukawa, V. P. Antropov, and Y. Singh, *Phys. Rev. B*, **84**, 094445 (2011).
 - ⁹ A. Pandey, R. S. Dhaka, J. Lamsal, Y. Lee, V. K. Anand, A. Kreyssig, T. W. Heitmann, R. J. McQueeney, A. I. Goldman, B. N. Harmon, A. Kaminski, and D. C. Johnston, *Phys. Rev. Lett.*, **108**, 087005 (2012).
 - ¹⁰ B. Saparov and A. S. Sefat, *Journal of Solid State Chemistry*, **204**, 32 (2013), ISSN 0022-4596.
 - ¹¹ T. G. Perring, R. A. Ewings, and J. V. Duijn, <http://horace.isis.rl.ac.uk> and unpublished.
 - ¹² D. L. Abernathy, M. B. Stone, M. J. Loguillo, M. S. Lucas, O. Delaire, X. Tang, J. Y. Y. Lin, and B. Fultz, *Review of Scientific Instruments*, **83**, 015114 (2012).
 - ¹³ R. J. McQueeney, S. O. Diallo, V. P. Antropov, G. D. Samolyuk, C. Broholm, N. Ni, S. Nandi, M. Yethiraj, J. L. Zarestky, J. J. Pulikkotil, A. Kreyssig, M. D. Lumsden, B. N. Harmon, P. C. Canfield, and A. I. Goldman, *Phys. Rev. Lett.*, **101**, 227205 (2008).
 - ¹⁴ J. Zhao, D.-X. Yao, S. Li, T. Hong, Y. Chen, S. Chang, W. Ratcliff, J. W. Lynn, H. A. Mook, G. F. Chen, J. L. Luo, N. L. Wang, E. W. Carlson, J. Hu, and P. Dai, *Phys. Rev. Lett.*, **101**, 167203 (2008).
 - ¹⁵ L. W. Harriger, H. Q. Luo, M. S. Liu, C. Frost, J. P. Hu, M. R. Norman, and P. Dai, *Phys. Rev. B*, **84**, 054544 (2011).
 - ¹⁶ S. O. Diallo, V. P. Antropov, T. G. Perring, C. Broholm, J. J. Pulikkotil, N. Ni, S. L. Bud'ko, P. C. Canfield, A. Kreyssig, A. I. Goldman, and R. J. McQueeney, *Phys. Rev. Lett.*, **102**, 187206 (2009).
 - ¹⁷ R. A. Ewings, T. G. Perring, R. I. Bewley, T. Guidi, M. J. Pitcher, D. R. Parker, S. J. Clarke, and A. T. Boothroyd, *Phys. Rev. B*, **78**, 220501 (2008).
 - ¹⁸ M. J. Han, Q. Yin, W. E. Pickett, and S. Y. Savrasov, *Phys. Rev. Lett.*, **102**, 107003 (2009).
 - ¹⁹ J. Zhao, D. T. Adroja, D.-X. Yao, R. Bewley, S. Li, X. F. Wang, G. Wu, X. H. Chen, J. Hu, and P. Dai, *Nat. Phys.*, **5**, 555 (2009).
 - ²⁰ K. Matan, R. Morinaga, K. Iida, and T. J. Sato, *Phys. Rev. B*, **79**, 054526 (2009).